Lecture 3

- Kinetic electron temperature, T_e
- Hydrogen recombination spectrum: the Balmer decrement
- Hβ recombination coefficient
- Mass determination from Hβ flux
- Emission-line chart
- Element abundance determinations
- BPT & VO diagrams

Atomic Energy Levels: O III ($1s^2 2s^2 2p^2$)

‘Permitted’ Selection Rules:

1. Outer electron must change (n, ℓ)
2. No spin change ($\Delta S = 0$)
3. ……….

Transition	Type	Wavelength	A_{21} (sec-1)	T_{exc} (°K)	n_e^{cr} (cm-3)
O III λ374	*Permitted (Resonance)*	Far-UV	10^9	10^5	10^{17}
O III] λ1663	*Intercombination*	UV	10^3	2×10^4	10^{11}
[O III] λ5007	*Forbidden*	Optical	10^{-1}	10^4	10^7
[O III] λ88μ	*Fine-structure (Forbidden)*	Far-IR	10^{-4}	10^2	10^3

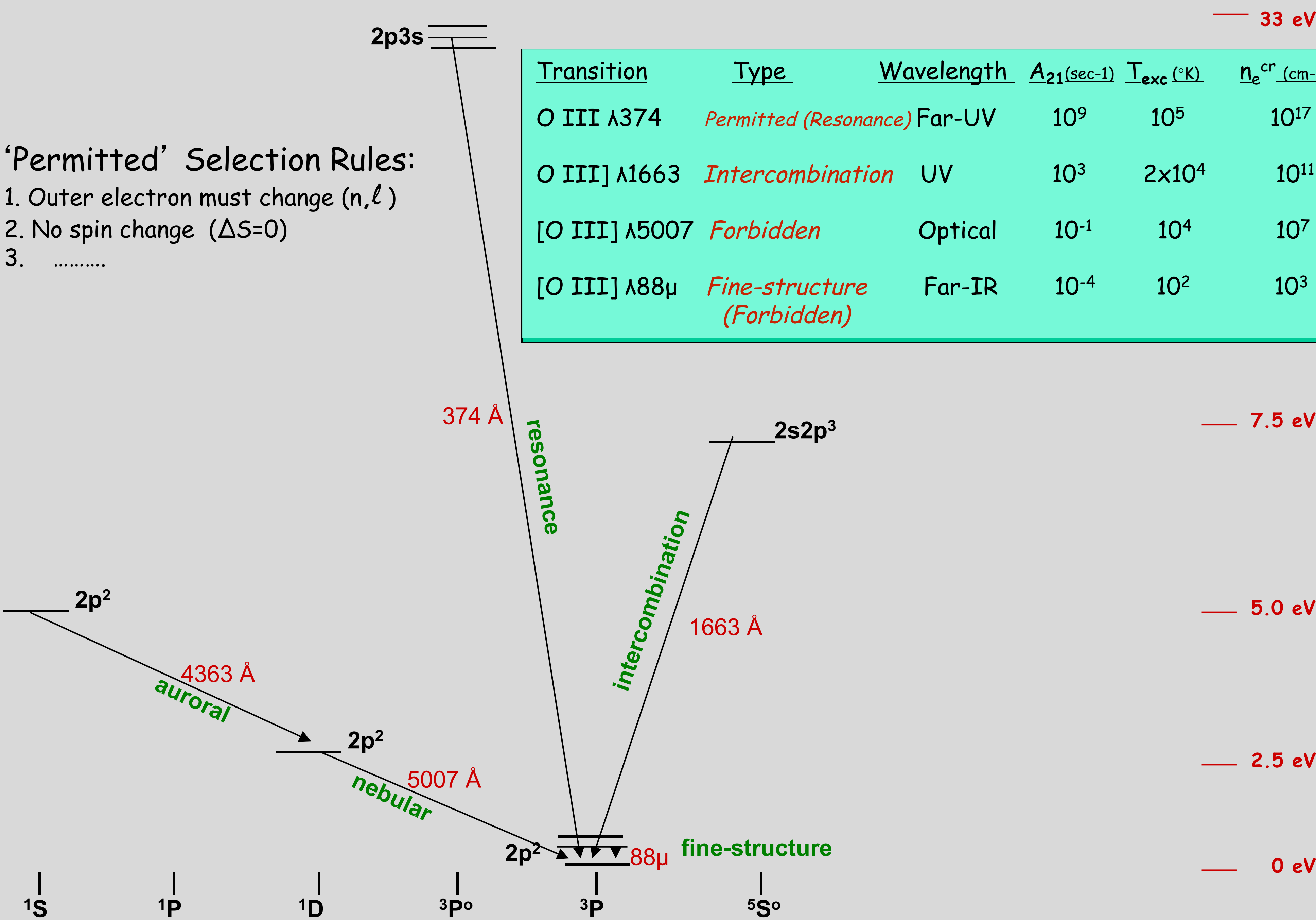

Plasma (ISM/IGM) Cooling Function

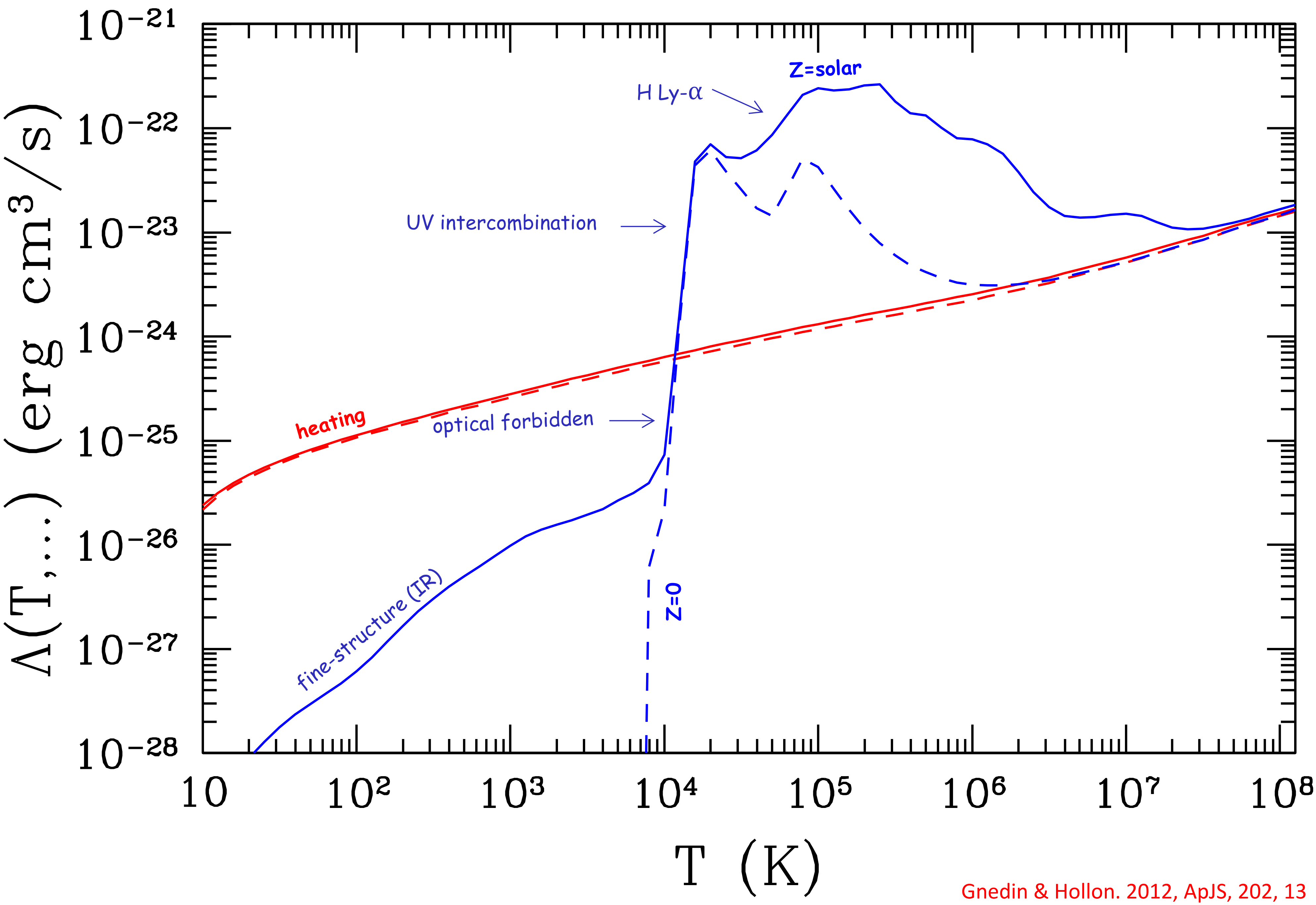

Gnedin & Hollon. 2012, ApJS, 202, 13

H Recombination Spectrum

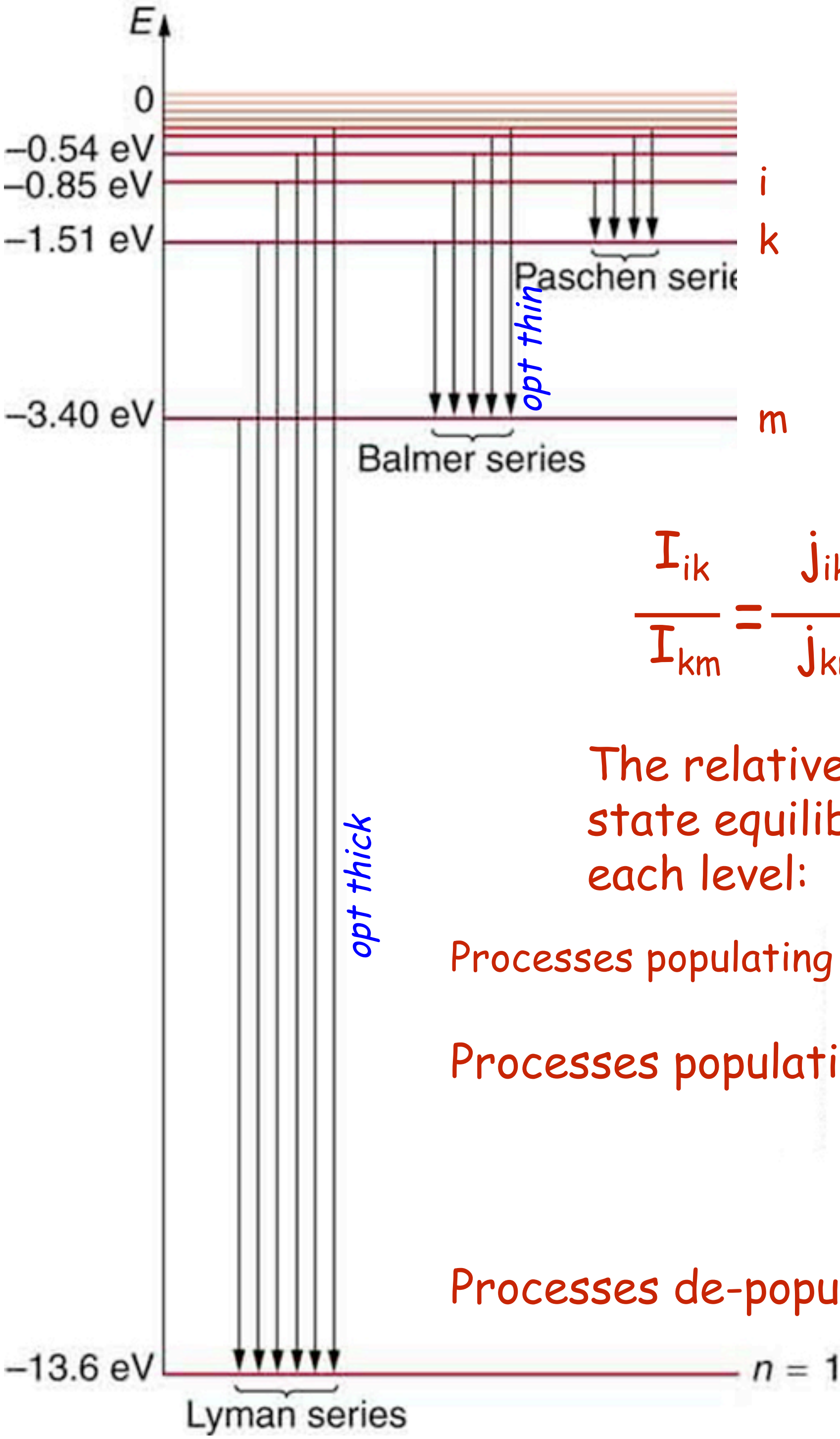

$$j_{ik} = n_i\, A_{ik}\, h\nu_{ik}/4\pi$$

For optically thin lines the relative intensities of H lines are given by:

$$\frac{I_{ik}}{I_{km}} = \frac{j_{ik}}{j_{km}} = \frac{n_i\, A_{ik}\, h\nu_{ik}}{n_k\, A_{km} h\nu_{km}} \propto \frac{n_i}{n_k}$$

The relative populations of levels are determined by steady-state equilibrium of processes that populate and de-populate each level:

Processes populating level k/(cm^{3}sec) = Processes de-populating level k/(cm^{3}sec)

$$\text{Processes populating k/(cm}^3\text{sec)} = n_e n_H \langle \underbrace{\sigma_k^{rec}(v)}_{\propto T_e^{-1/2}}\, v\rangle + n_i \sum_{i>k} A_{ik}$$

$$\text{Processes de-populating k/(cm}^3\text{sec)} = n_k \sum_{m<k} A_{km}$$

H Recombination Lines

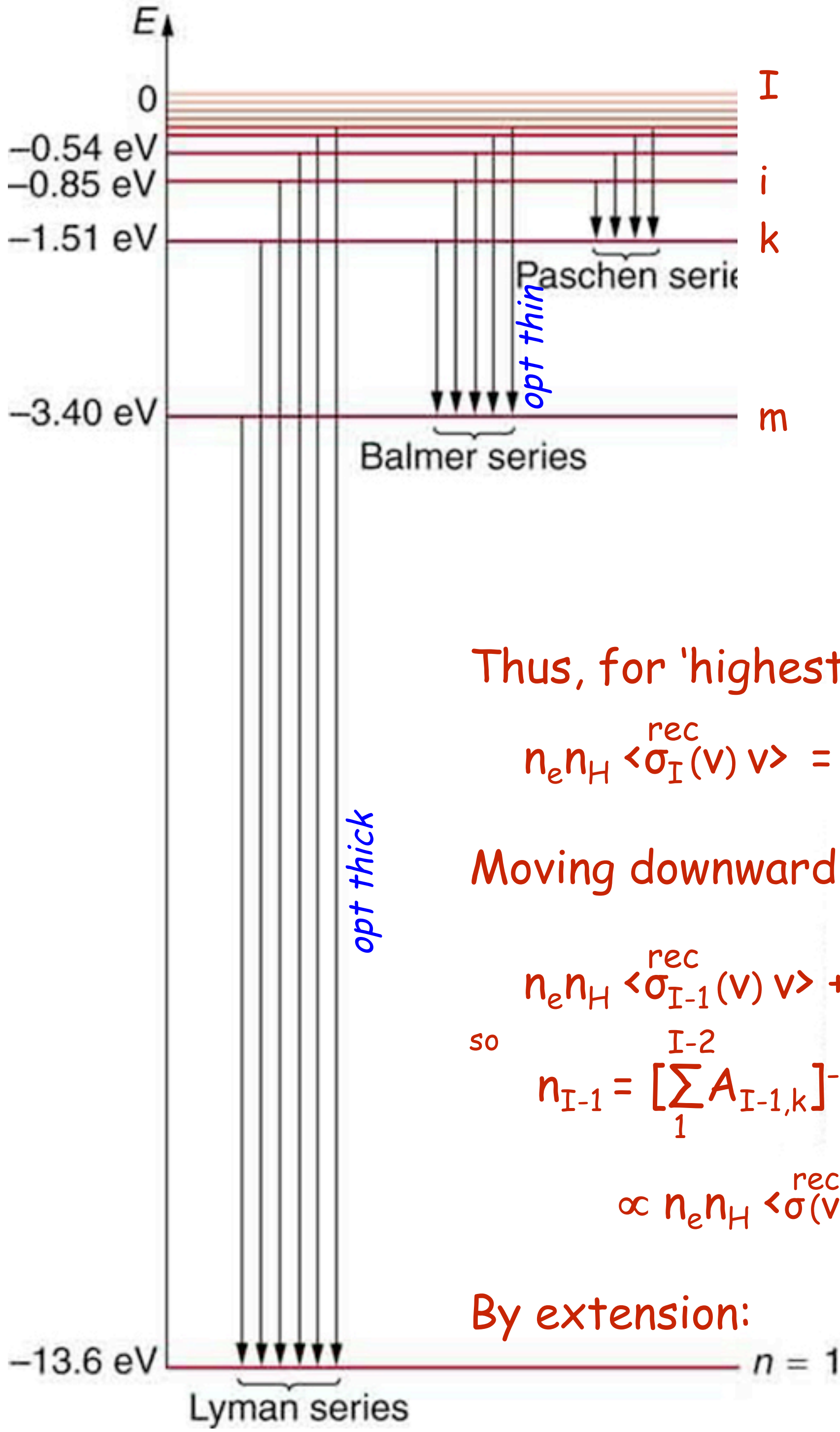

Thus, for level k:

$$n_e n_H \langle \sigma_k^{rec}(v)\, v\rangle + n_i \sum_{i>k} A_{ik} = n_k \sum_{m<k} A_{km}$$

(m=1 or 2?) Case A: m=1; Case B: m=2)

These coupled "Capture-cascade Equations" can be solved for the relative populations n_k of the many H levels. A practical way to solve them for a finite number of levels is to arbitrarily define a highest level I that is many levels above the level of interest, and solve for n_k working downward.

Thus, for 'highest' level I there are no levels above it. So,

$$n_e n_H \langle \sigma_I^{rec}(v)\, v\rangle = n_I \sum_{1}^{I-1} A_{Ik} \longrightarrow n_I = \left[\sum_{1}^{I-1} A_{Ik}\right]^{-1} \times n_e n_H \langle \sigma_I^{rec}(v)\, v\rangle \propto n^2\, T_e^{-1/2}$$

Moving downward to solve for the next lower level I-1, one has

$$n_e n_H \langle \sigma_{I-1}^{rec}(v)\, v\rangle + n_I A_{I,I-1} = n_{I-1} \sum_{1}^{I-2} A_{I-1,k}$$

so

$$n_{I-1} = \left[\sum_{1}^{I-2} A_{I-1,k}\right]^{-1} \times \left[n_e n_H \langle \sigma_{I-1}^{rec}(v)\, v\rangle + \underbrace{n_I A_{I,I-1}}_{\propto n_e n_H \langle \sigma_I(v)\, v\rangle}\right]$$

$$\propto n_e n_H \langle \sigma^{rec}(v)\, v\rangle \propto n^2\, T_e^{-1/2}$$

By extension: $\boxed{n_k = n_e n_H\, f_k(T_e) \propto n^2\, T_e^{-1/2}}$

The Balmer Decrement

Based on the results of the Capture-cascade equations the relative intensities of any 2 optically thin H emission lines can be written

$$\frac{I_{ik}}{I_{km}} = \frac{j_{ik}}{j_{km}} = \frac{n_i A_{ik} h\nu_{ik}}{n_k A_{km} h\nu_{km}} \propto \frac{n^2 f_i(T_e)}{n^2 f_k(T_e)} \propto \frac{T_e^{-1/2}}{T_e^{-1/2}} = \text{const.}$$

Therefore, the relative intensities of H lines are independent of both density and temperature. The relative intensities of the Balmer lines (transitions to level 2) is called the Balmer decrement and has been calculated by solving the capture-cascade equations.

	5000° K		10,000° K			20,000° K	
N_e (cm^{-3})	10^2	10^4	10^2	10^4	10^6	10^2	10^4
$4\pi j_{H\beta}/N_p N_e$ (erg cm^3 sec^{-1})	2.20×10^{-25}	2.22×10^{-25}	1.24×10^{-25}	1.24×10^{-25}	1.25×10^{-25}	0.658×10^{-25}	0.659×10^{-25}
$\alpha^{eff}_{H\beta}$ (cm^3 sec^{-1})	5.38×10^{-14}	5.44×10^{-14}	3.02×10^{-14}	3.03×10^{-14}	3.07×10^{-14}	1.61×10^{-14}	1.61×10^{-14}
Balmer-line intensities relative to $H\beta$							
$j_{H\alpha}/j_{H\beta}$	3.04	3.00	2.86	2.85	2.81	2.75	2.74
$j_{H\gamma}/j_{H\beta}$	0.458	0.460	0.468	0.469	0.471	0.475	0.476
$j_{H\delta}/j_{H\beta}$	0.251	0.253	0.259	0.260	0.262	0.264	0.264
$j_{H\epsilon}/j_{H\beta}$	0.154	0.155	0.159	0.159	0.163	0.163	0.163
$j_{H8}/j_{H\beta}$	0.102	0.102	0.105	0.105	0.110	0.107	0.107
$j_{H9}/j_{H\beta}$	0.0709	0.0714	0.0731	0.0734	0.0786	0.0746	0.0746
$j_{H10}/j_{H\beta}$	0.0515	0.0520	0.0530	0.0533	0.0590	0.0540	0.0541
$j_{H15}/j_{H\beta}$	0.0153	0.0163	0.0156	0.0162	0.0214	0.0158	0.0161
$j_{H20}/j_{H\beta}$	0.0066	0.0082	0.0066	0.0075	0.0105	0.0066	0.0072
Paschen-line intensities relative to corresponding Balmer lines							
$j_{P\alpha}/j_{H\beta}$	0.410	0.396	0.338	0.332	0.317	0.284	0.281
$j_{P\beta}/j_{H\gamma}$	0.402	0.396	0.348	0.345	0.335	0.305	0.305
$j_{P\gamma}/j_{H\delta}$	0.393	0.388	0.349	0.346	0.339	0.312	0.311
j_{P8}/j_{H8}	0.382	0.381	0.348	0.348	0.333	0.317	0.316
j_{P10}/j_{H10}	0.379	0.377	0.347	0.345	0.325	0.318	0.316
j_{P15}/j_{H15}	0.375	0.363	0.347	0.339	0.313	0.319	0.315
j_{P20}/j_{H20}	0.371	0.346	0.346	0.327	0.309	0.320	0.309
Brackett-line intensities relative to corresponding Balmer lines							
$j_{Br\alpha}/j_{H\gamma}$	0.227	0.215	0.171	0.166	0.154	0.132	0.127
$j_{Br\beta}/j_{H\delta}$	0.222	0.214	0.175	0.172	0.163	0.141	0.140
$j_{Br\gamma}/j_{H\epsilon}$	0.214	0.209	0.175	0.173	0.163	0.144	0.143
$j_{Br\delta}/j_{H8}$	0.209	0.206	0.174	0.172	0.160	0.146	0.145
j_{Br10}/j_{H10}	0.204	0.200	0.172	0.170	0.152	0.146	0.146
j_{Br15}/j_{H15}	0.197	0.186	0.170	0.164	0.137	0.147	0.143
j_{Br20}/j_{H20}	0.193	0.169	0.169	0.154	0.133	0.147	0.138

Osterbrock, AGN[2], p. 84

Hβ Recombination Coefficient

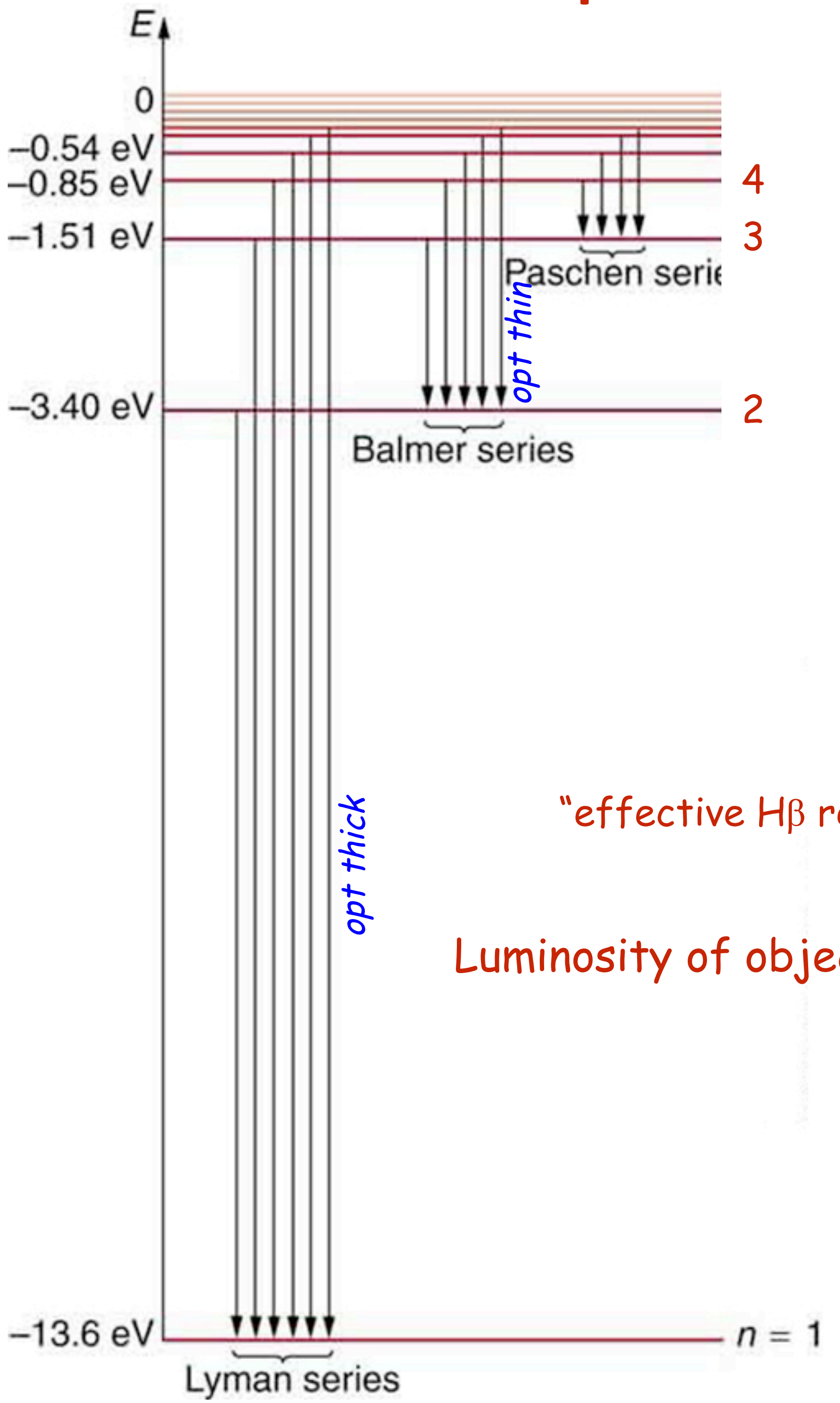

For n=4 of hydrogen can write

$$n_4 = n_e n_H \, f_4(Te)$$

Thus, for the Balmer Hβ line (4 ->2), which is the ***standard reference emission feature in most spectra***, we can write the emission coefficient

$$j_{H\beta} = n_4 \, A_{42} \, h\nu_{42}/4\pi \; = n_e n_H \, f_4(Te) \, A_{42} \, h\nu_\beta/4\pi$$

$$= n_e n_H \underbrace{f_4(Te) \, A_{42}}_{||} \, h\nu_\beta/4\pi$$

"effective Hβ recombination coefficient", $\alpha^{rec}_{H\beta}(T_e) = 3.0\text{x}10^{-14}\ \text{cm}^3\ \text{s}^{-1}$

Luminosity of object in Hβ, $L_{H\beta} = \int (4\pi j_{H\beta}) \, dV$ ergs/sec (optically thin)

$$= \alpha^{eff}_{H\beta} \, h\nu_\beta \int n_e n_H \, dV$$

$$= 4\pi d^2 \, F_{H\beta}$$ $\longleftarrow$ observed flux

Mass from Hβ Flux & Mean Density

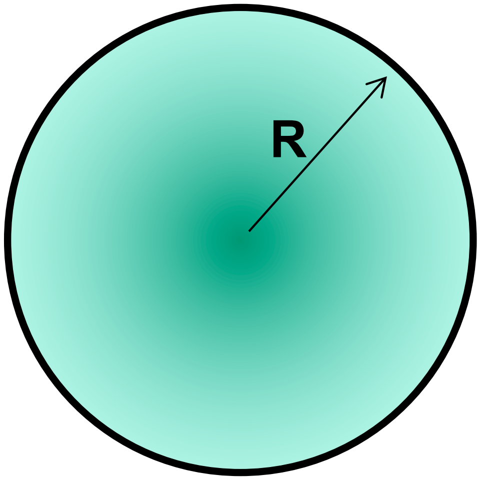

An approximate object mass may be derived from the observed Hβ flux of an object:

Luminosity of object $$L_{H\beta} = \int (4\pi j_{H\beta})\, dV = \alpha_{H\beta}\, h\nu_\beta \int_{vol} n_e n_H\, dV$$

$$= 4\pi d^2 F_{H\beta}$$

$$\text{Mass, } \mathcal{M} = \int_{vol} m_H n_H\, dV$$

Suppose a mean $\langle n_e \rangle$ is determined from forbidden line intensity ratios. Then,

$$\text{Mass, } \boxed{\mathcal{M} = \frac{4\pi m_H\, d^2 F_{H\beta}}{\alpha_{H\beta}\, h\nu_\beta \langle n_e \rangle}}$$

Many emission objects (PNe, extragalactic H II regions, SNR, etc.) have masses determined this way from known distance d, observed Hβ flux, and mean density $\langle n_e \rangle$ derived from forbidden line intensity ratios.

For objects that are homogeneous in density, the derived mass may be reliable to <50%. But, if there are unknown density inhomogeneities, the derived mass may be in error by more than a factor of 10-50.

Low-lying Levels of Heavy Elements

Electron Configuration: 2p   Terms: ^2P

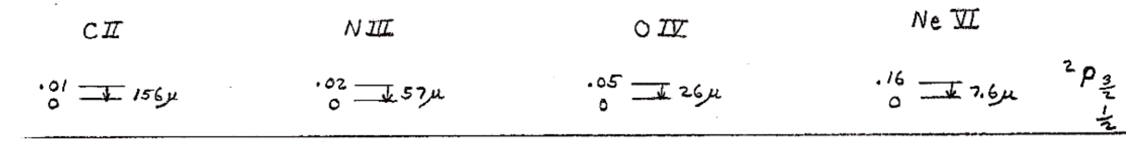

Electron Configuration: $2p^2$ Terms: ^3P, ^1D, ^1S

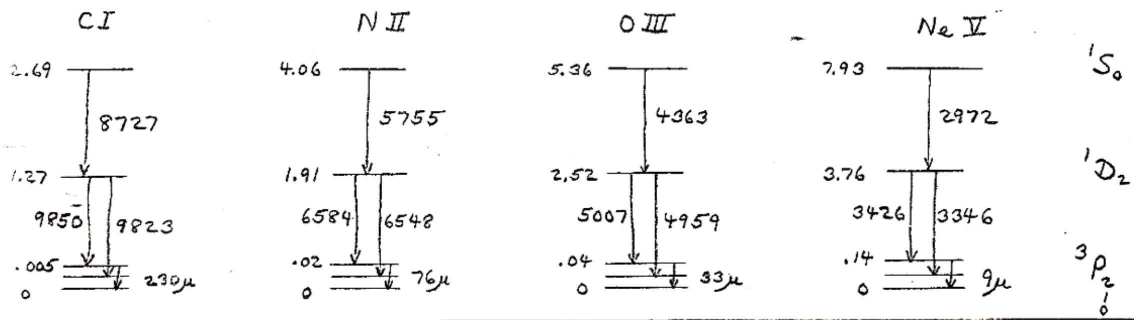

Electron Configuration: $2p^3$ Terms: ^4S, ^2D, ^2P

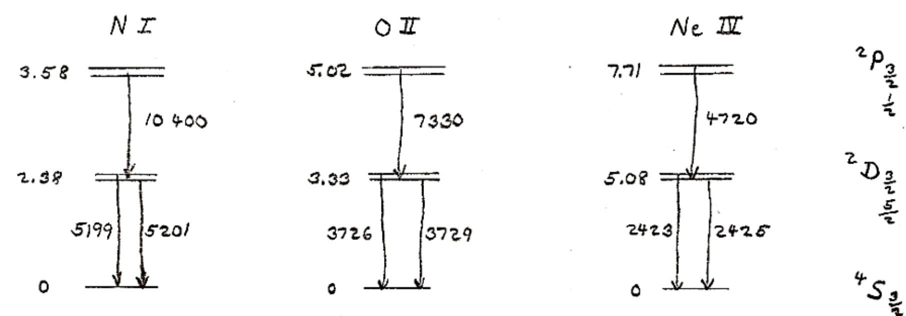

Electron Configuration: $2p^4$ Terms: ^3P, ^1D, ^1S

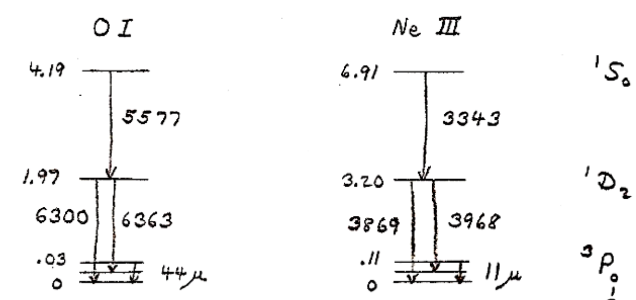

Electron Configuration: $2p^5$ Terms: ^2P

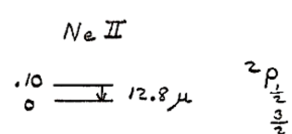

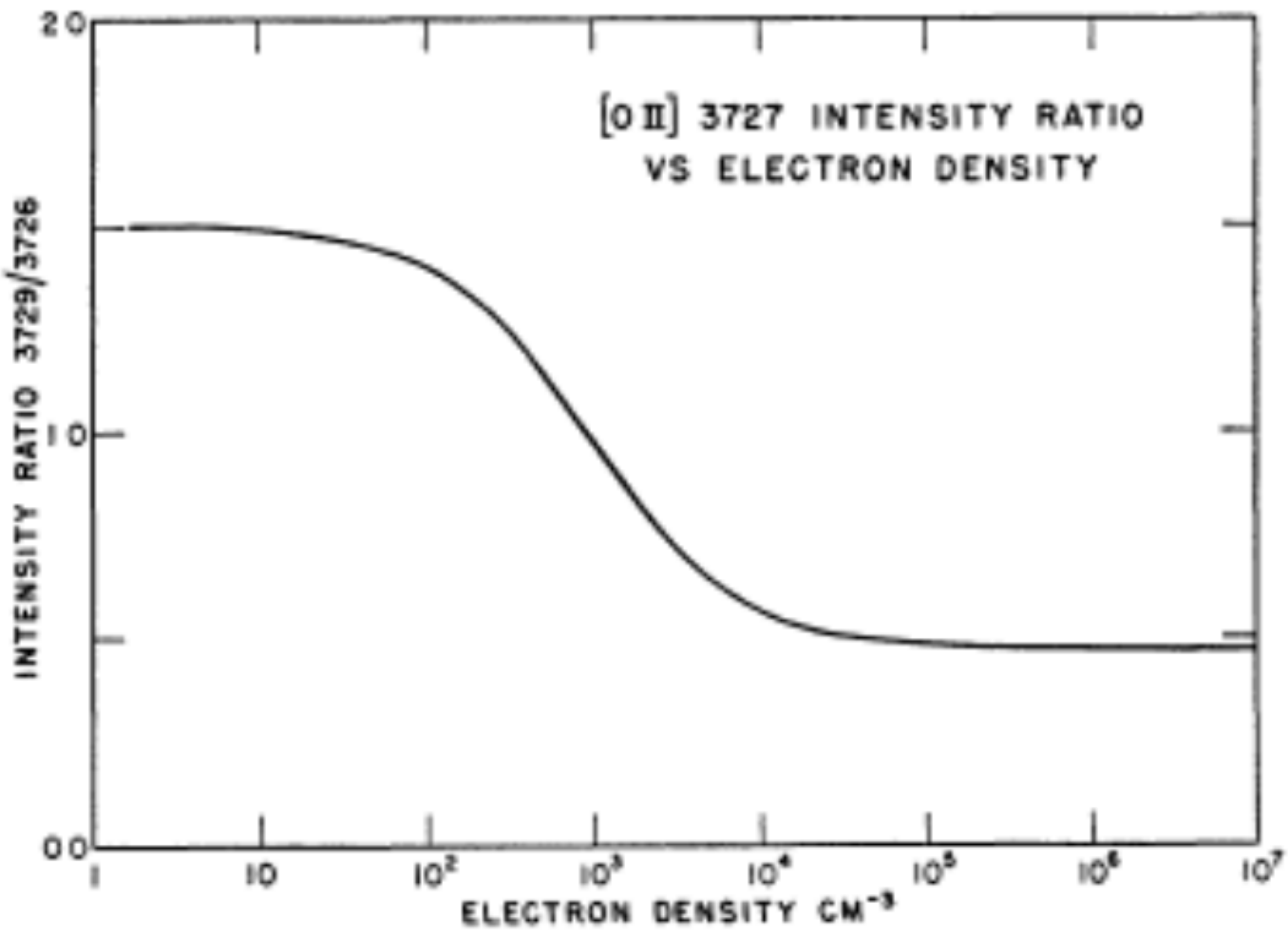

FIG. 1. Variation of λ 3729/λ 3726 intensity ratio with electron temperature at 10,000° K

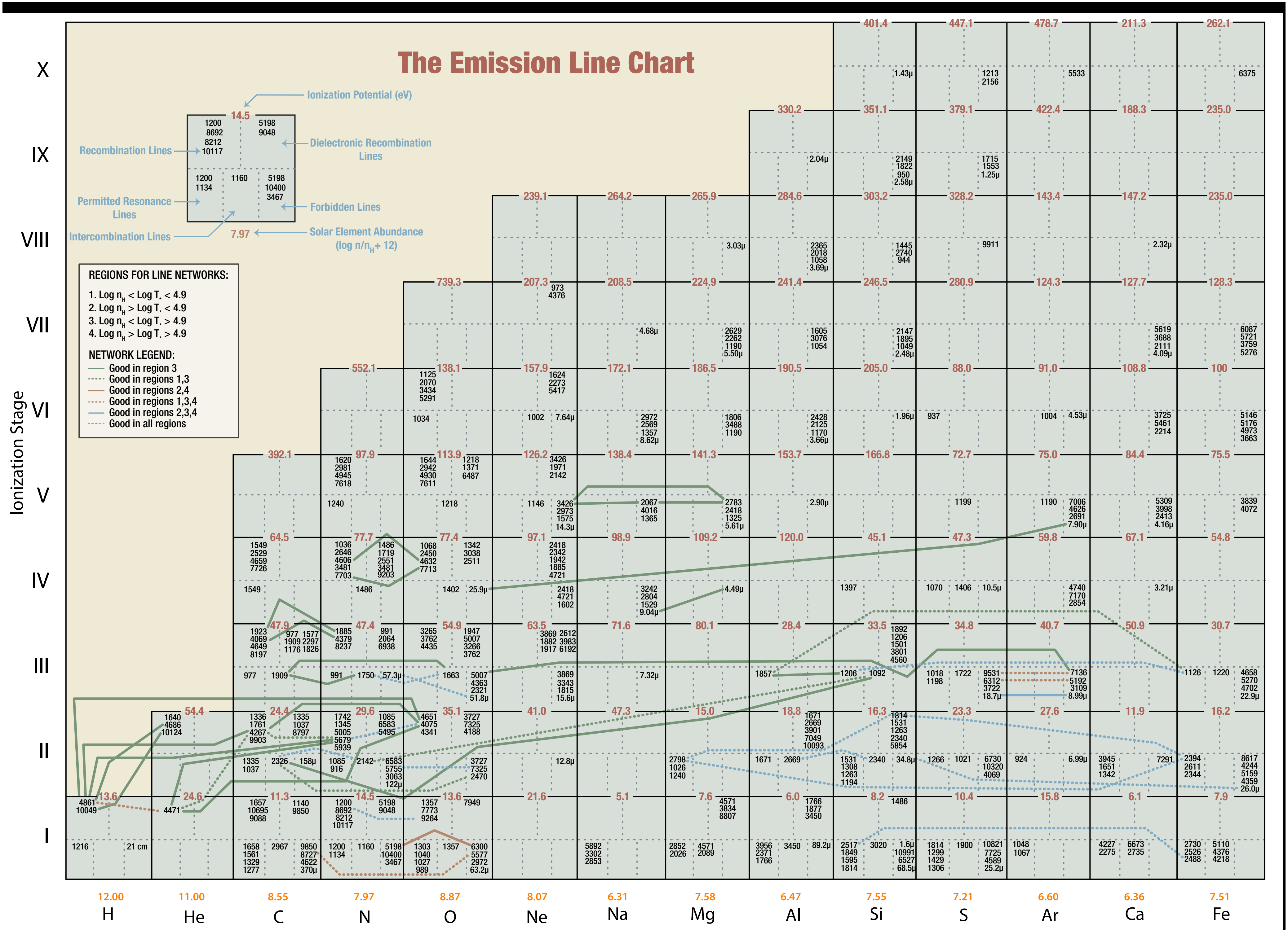

Kingdon & Williams. 1997, AJ. 113, 2193

Atomic Energy Levels: O III ($1s^2 2s^2 2p^2$)

'Permitted' Selection Rules:

1. Outer electron must change (n, ℓ)
2. No spin change ($\Delta S=0$)
3. ....

Transition	Type	Wavelength	A_{21} (sec-1)	T_{exc} (°K)	n_e^{cr} (cm-3)
O III λ374	*Permitted (Resonance)*	Far-UV	10^9	10^5	10^{17}
O III] λ1663	*Intercombination*	UV	10^3	2×10^4	10^{11}
[O III] λ5007	*Forbidden*	Optical	10^{-1}	10^4	10^7
[O III] λ88μ	*Fine-structure (Forbidden)*	Far-IR	10^{-4}	10^2	10^3

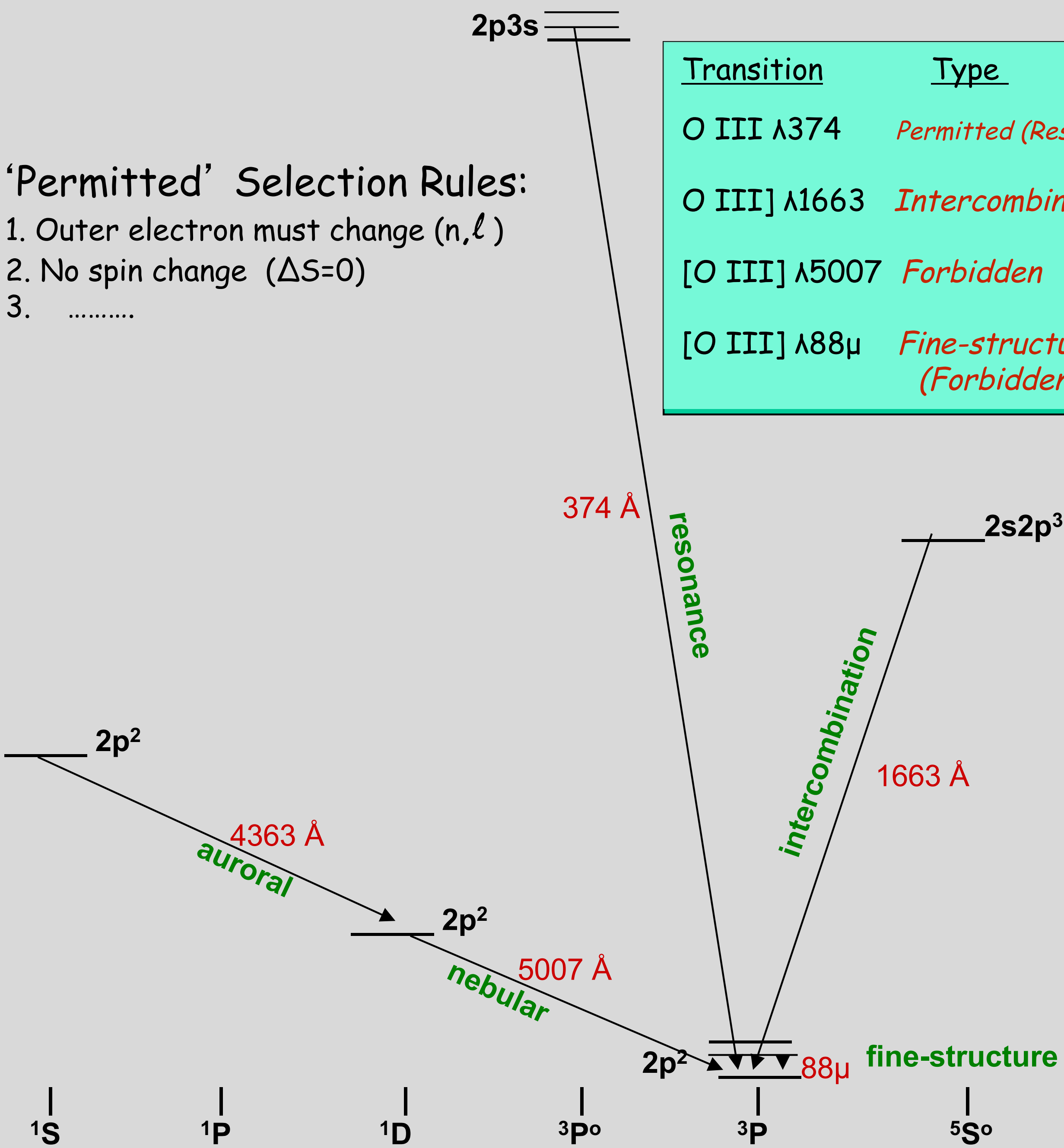

Bashkin & Stoner. 1975, Atomic Energy Levels (North Holland)

Element Abundances from Emission Spectra

- Abundances are determined from relative line intensities:

$$\frac{I_{ij}}{I_{mn}} \propto \frac{\int j_{ij}\, d\ell}{\int j_{mn}\, d\ell} \propto \frac{\int n_i A_{ij} h\nu_{ij}\, d\ell}{\int n_m A_{mn} h\nu_{mn}\, d\ell}$$

Therefore, one must determine ***integrated*** ion abundances ***along the line of sight***. This can be done in two ways: (1) build a model ionized region using codes like 'CLOUDY' or 'MAPPINGS' and calculate expected intensities to compare with observations, or (2) select two ions that occupy the same space (because they have the same ionization potentials) and assume the element abundances to be the same as the ion abundance ratio, e.g., $N^+/O^+ = N/O$.

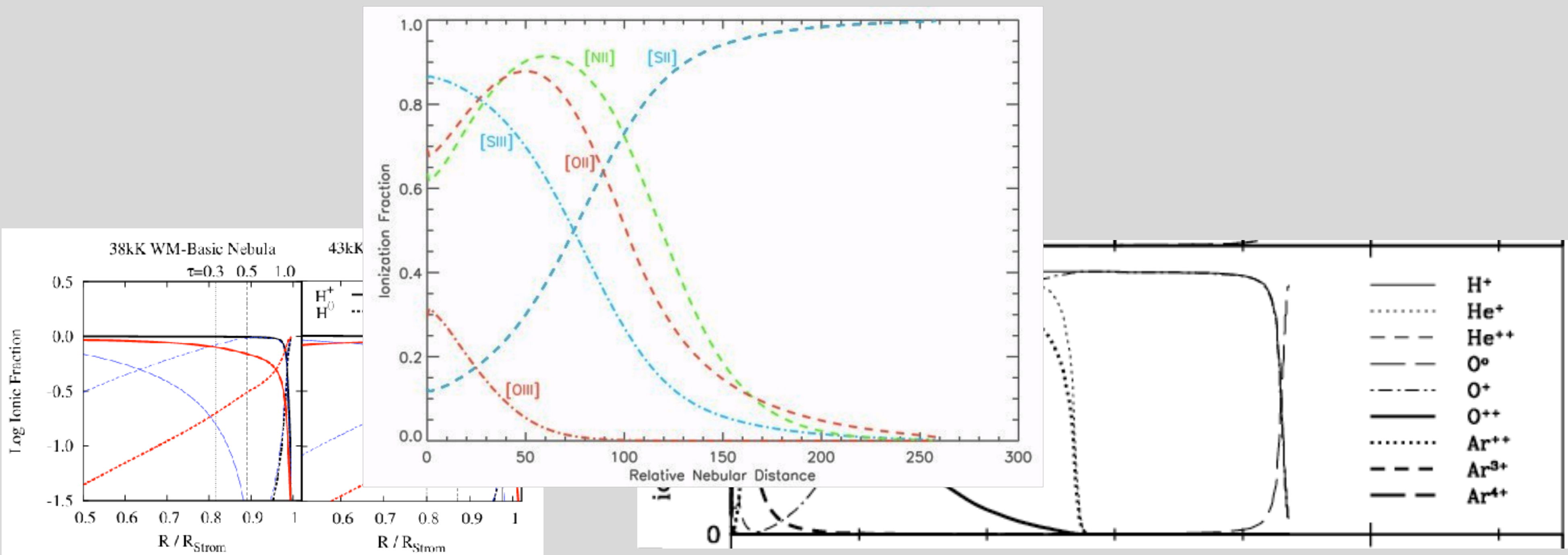

Planetary Nebula

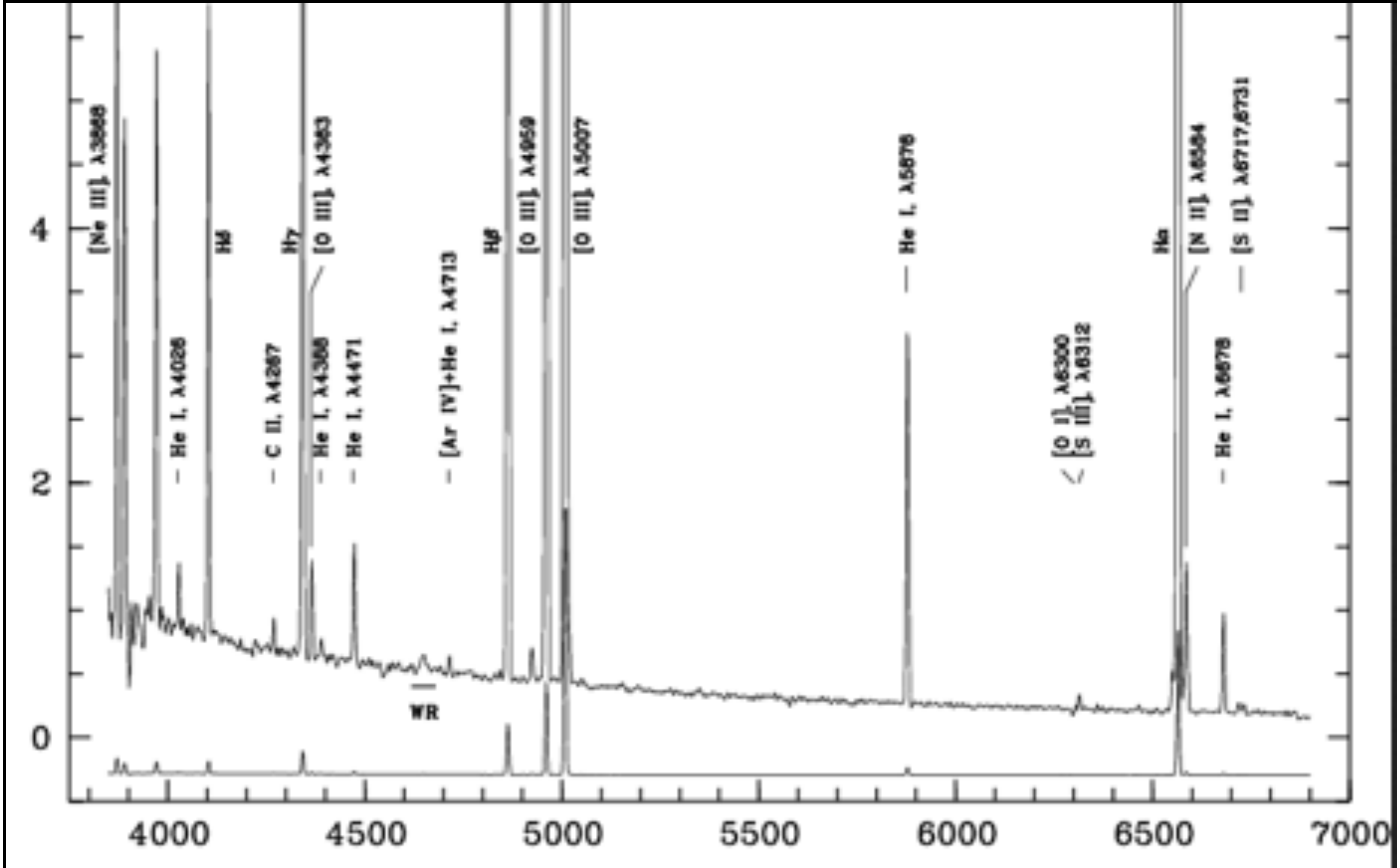

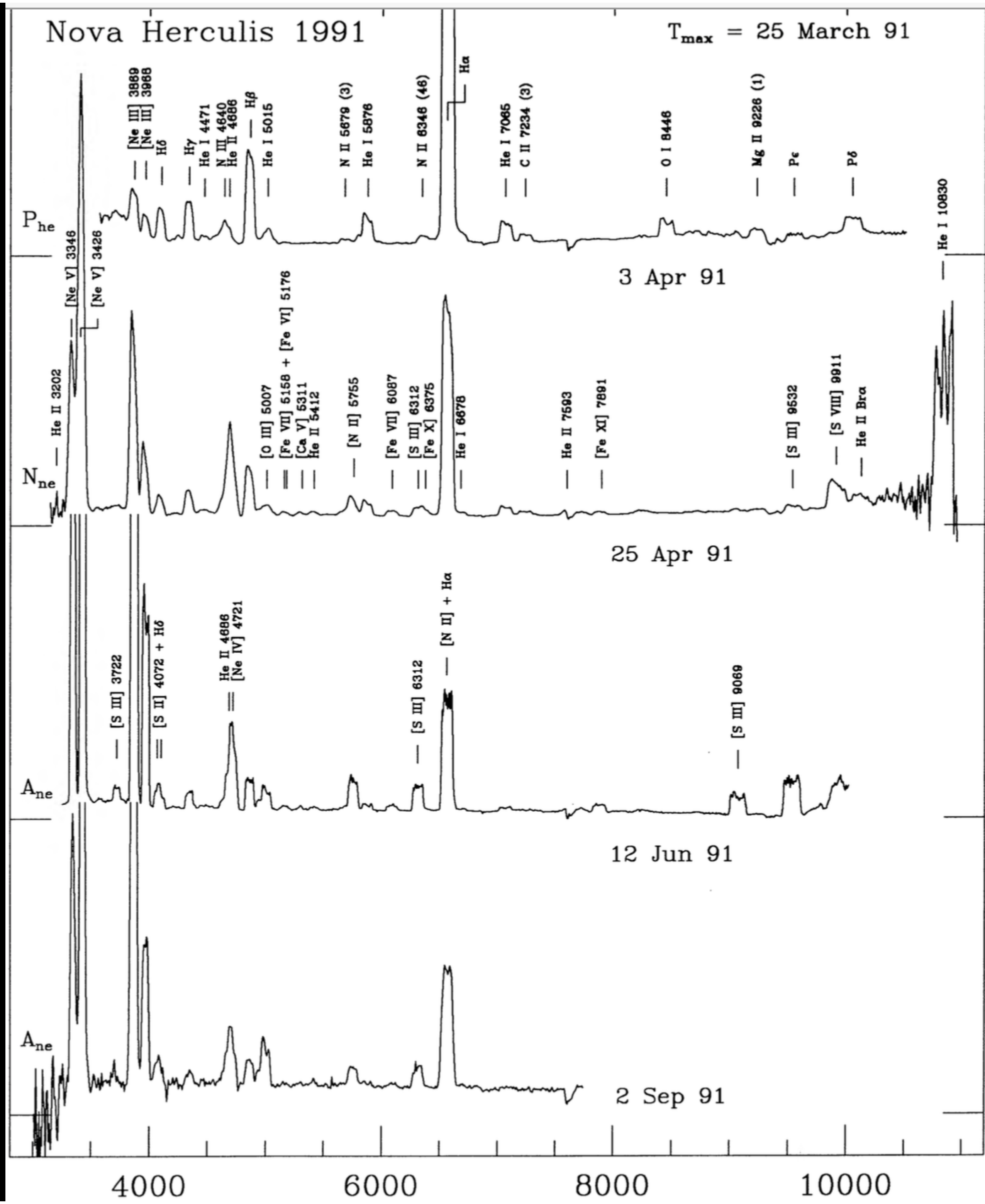

Nova Herculis 1991
T_{max} = 25 March 91
3 Apr 91
25 Apr 91
12 Jun 91
2 Sep 91
P_{he}
N_{ne}
A_{ne}
A_{ne}
[Ne III] 3869
[Ne III] 3968
Hδ
Hγ
He I 4471
N III 4640
He II 4686
Hβ
He I 5015
N II 5679 (3)
He I 5876
N II 6346 (46)
Hα
He I 7065
C II 7234 (3)
O I 8446
Mg II 9226 (1)
Pε
Pδ
He I 10830
[Ne V] 3346
[Ne V] 3426
He II 3202
[O III] 5007
[Fe VII] 5158 + [Fe VI] 5176
[Ca V] 5311
He II 5412
[N II] 5755
[Fe VII] 6087
[S III] 6312
[Fe X] 6375
He I 6678
He II 7593
[Fe XI] 7891
[S III] 9532
[S VIII] 9911
He II Brα
[S III] 3722
[S II] 4072 + Hδ
He II 4686
[Ne IV] 4721
[S III] 6312
[N II] + Hα
[S III] 9069
4000
6000
8000
10000

Element Abundances from Emission Spectra (cont'd)

- A third alternative for ionized regions is (3) determine relative abundances of all the ions of an element, add them together and compare their abundance with that of H in the ionized gas.

Oxygen does have lines from the first three ionization stages visible in the optical: [O I] λ6300, [O II] λ3727, & [O III] λ5007. Their intensities reveal their relative abundances w.r.t. hydrogen. Correcting for (or ignoring) the presence of unobserved O^{+3}, O^{+4}, etc, one can write

$$\frac{O}{H} \propto \frac{\overset{\text{(neutral)}}{F\,[O\ I]} + F\,[O\ II] + F\,[O\ III]}{F\,(H\beta)}$$

called 'R23' method

Pagel, B. et al. 1979, MNRAS, 189, 95

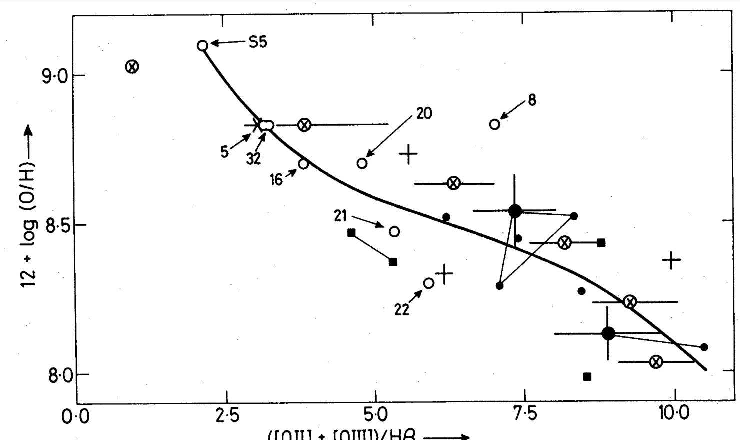

Figure 7. Oxygen abundance plotted against ([O II] + [O III])/Hβ, with symbols as in Figs 5 and 6, except that the circled crosses on this diagram represent points taken from the sequence of dusty models by Sarazin. The horizontal error bars attached to these straddle the range from his sequence A (right) to his sequence B (left).

EVIDENCE FOR COMPOSITION GRADIENTS ACROSS THE DISKS OF SPIRAL GALAXIES

LEONARD SEARLE
Hale Observatories, Carnegie Institution of Washington, California Institute of Technology
Received 1971 April 7

ABSTRACT

The integrated spectra of H II regions located in the inner spiral arms of Sc galaxies are systematically different from those of H II regions in the outer arms. This is, in part at least, an abundance effect. The N/O ratio (and probably also the abundance ratios O/H and N/H) decreases from the inner to the outer arms.

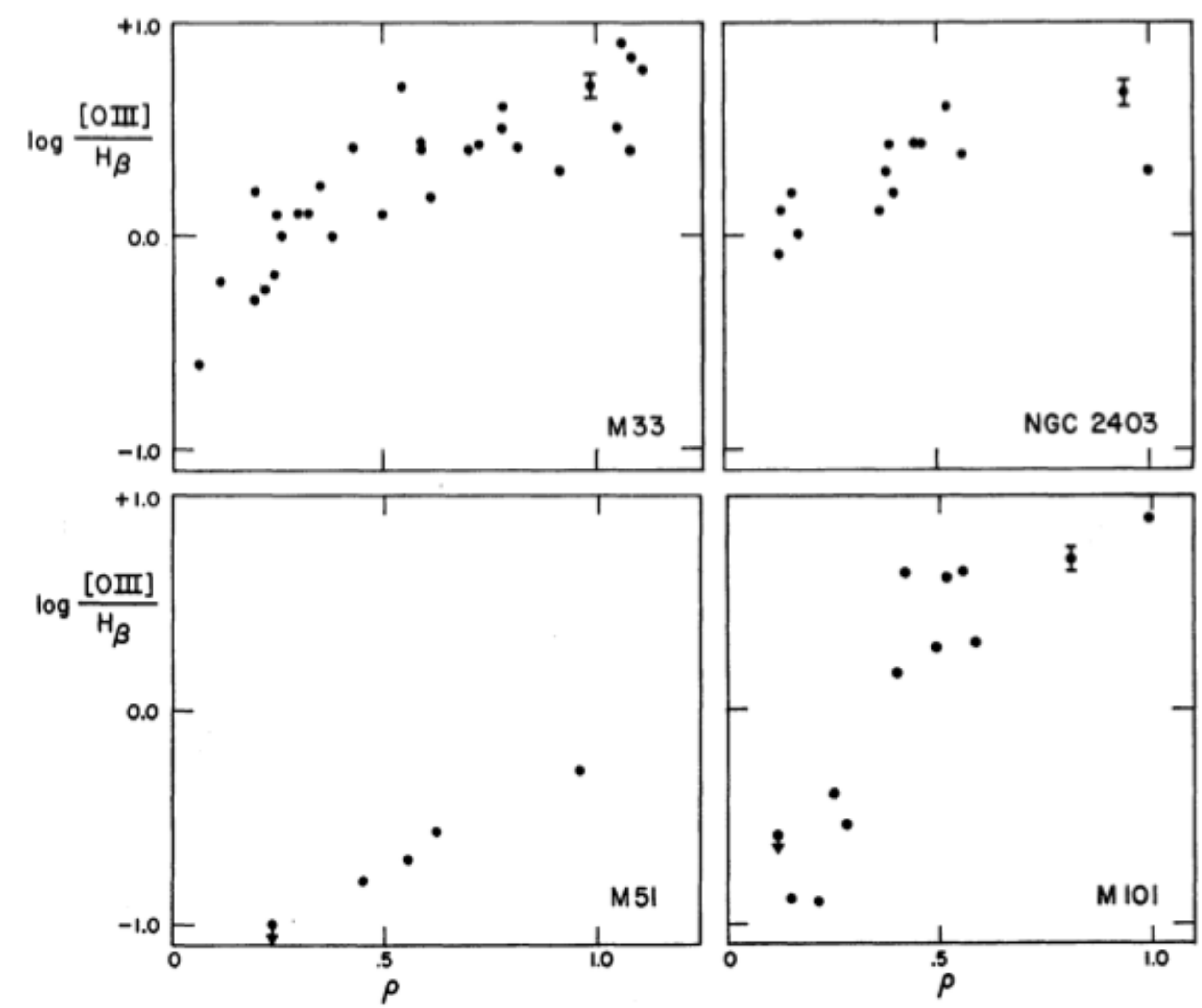

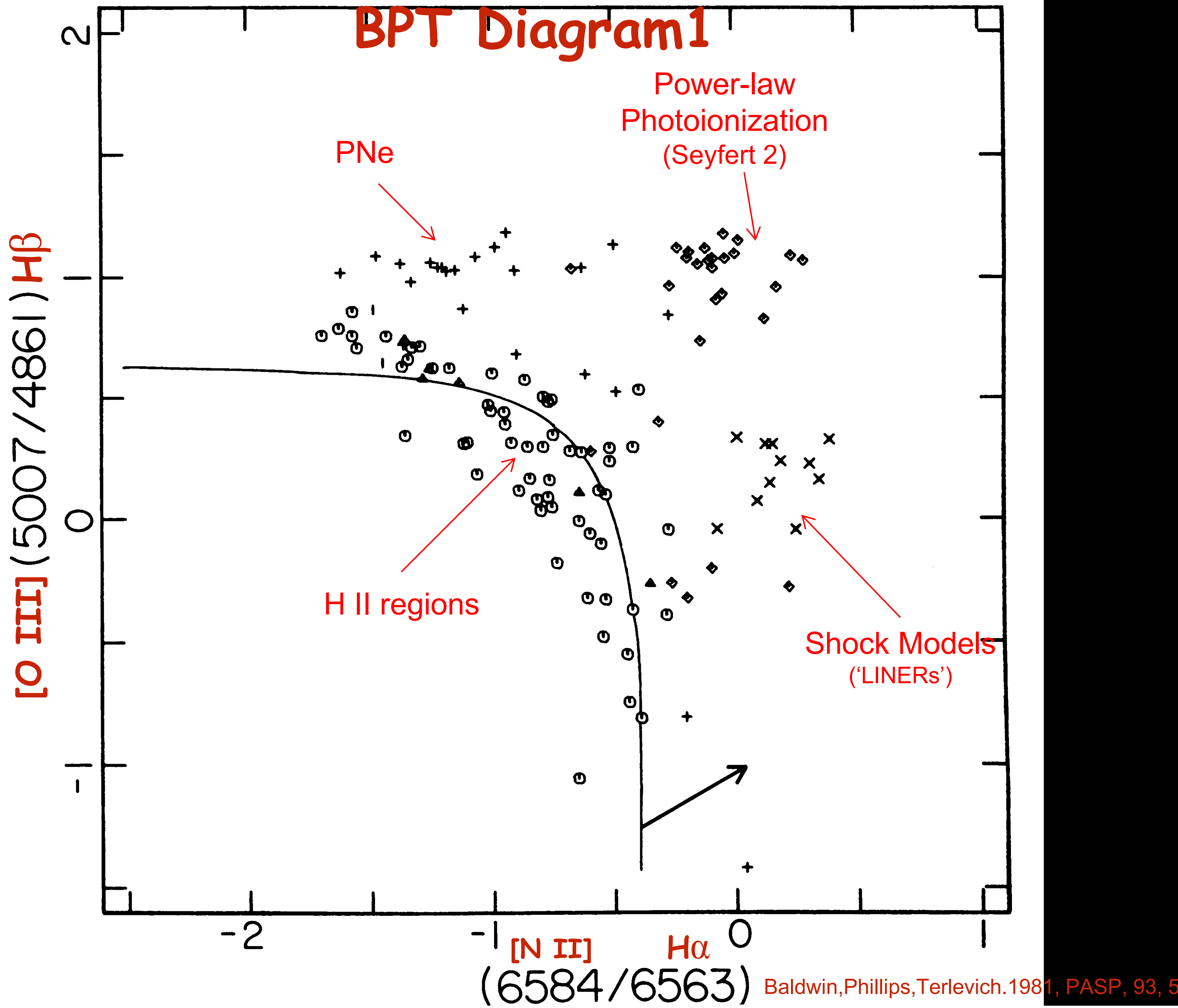
BPT Diagram1
Power-law
Photoionization
(Seyfert 2)
PNe
H II regions
Shock Models
('LINERs')
[O III] (5007/4861) Hβ
[N II] Hα (6584/6563)
-2
-1
0
1
2
Baldwin,Phillips,Terlevich.1981, PASP, 93, 5

BPT Diagram2

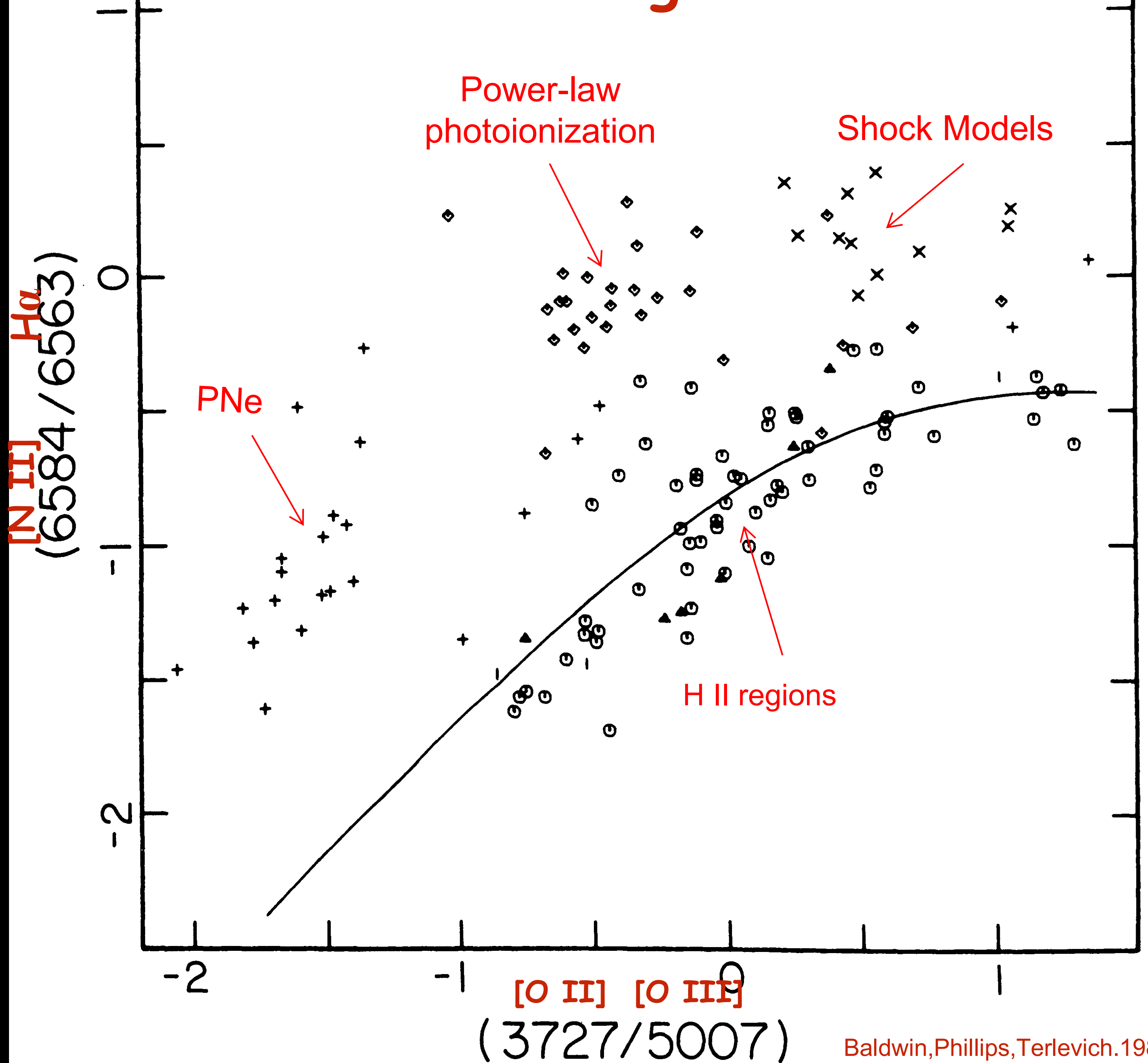

Baldwin,Phillips,Terlevich.1981, PASP, 93, 5

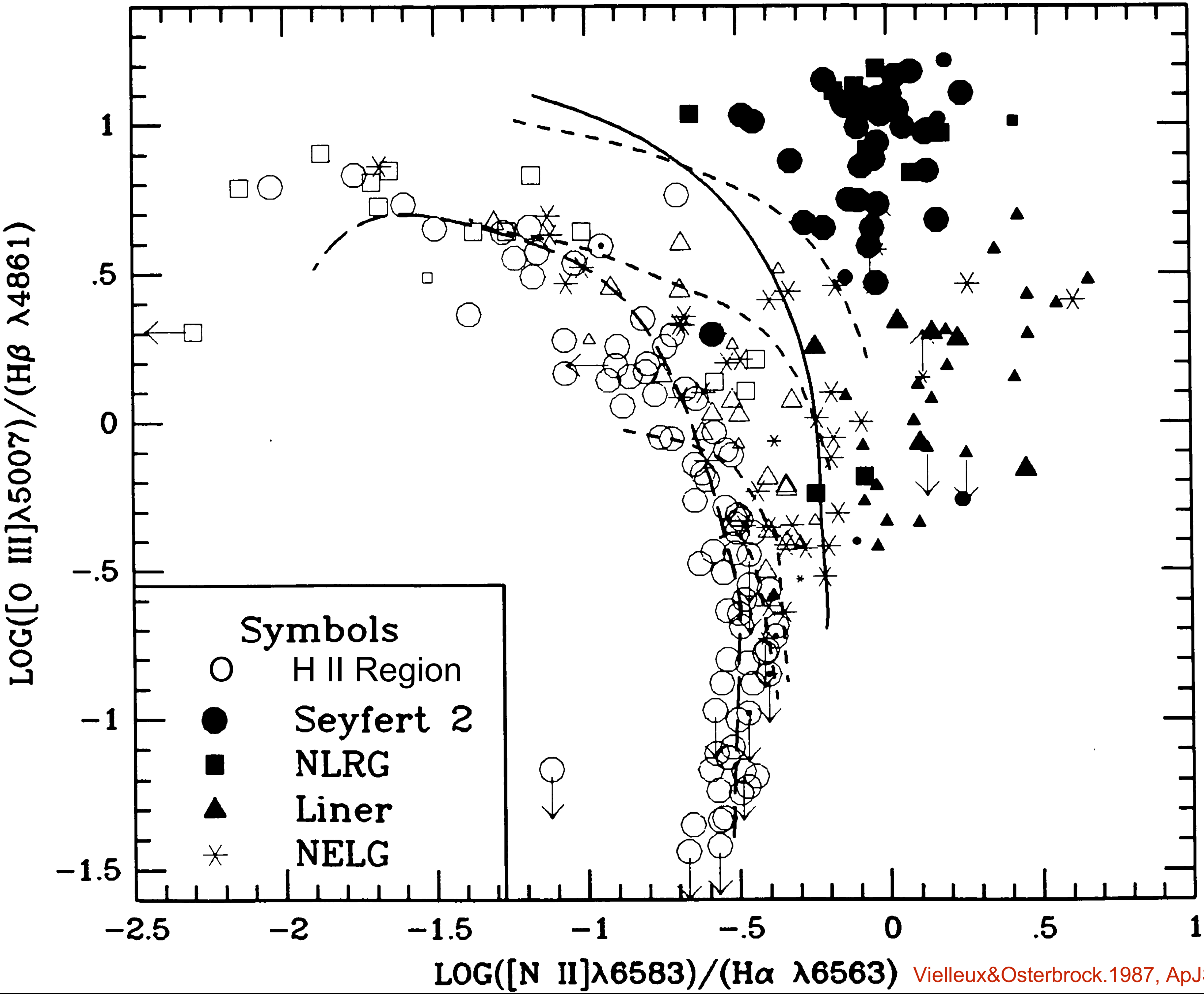

Vielleux&Osterbrock.1987, ApJS,63,295

BPT Diagram for Galaxies

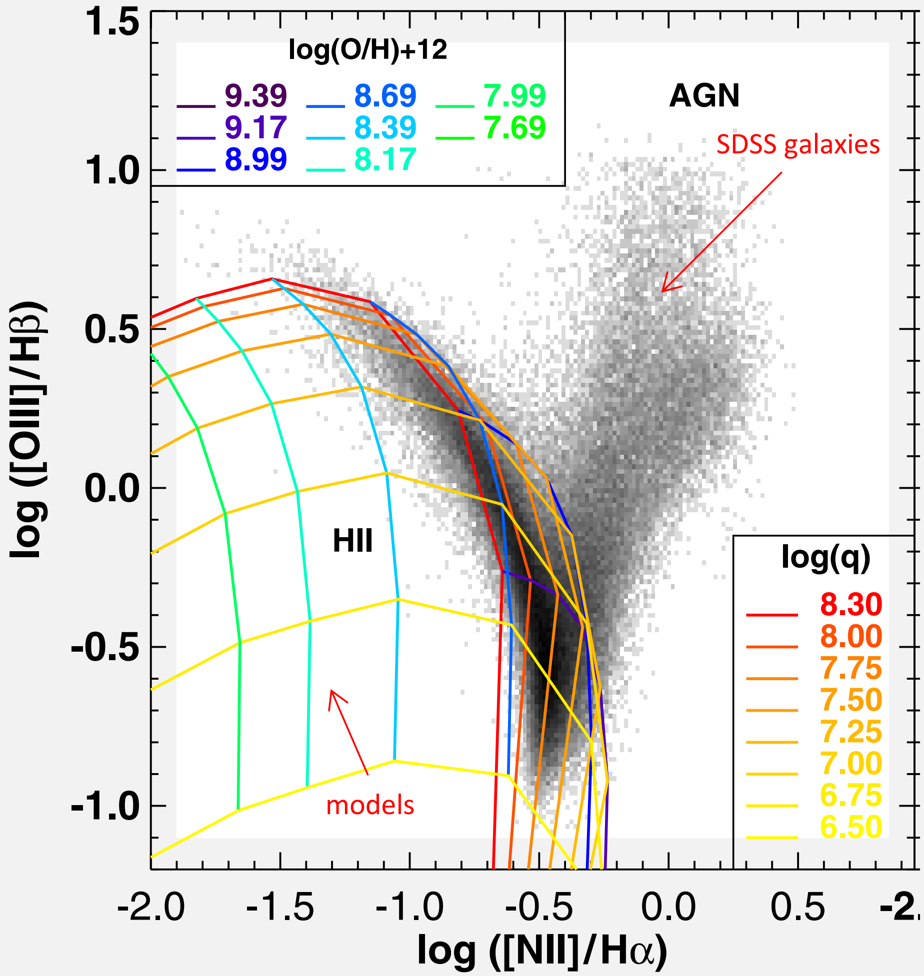

"The position of our theoretical star-forming galaxy abundance sequence is determined by: (1) the shape of the ionizing radiation field, (2) the geometrical distribution of gas with respect to the ionizing sources, (3) the metallicity range, and (4) the electron density (pressure) of the gas."

Kewley et al. 2013, ApJ, 774, 100